Research Article

Fluoride uptake by human tooth enamel: Topical application versus combined dielectrophoresis and AC electroosmosis

CHRIS S. IVANOFF, DDS, **BASHIR I. MORSHED**, MS, PHD, **TIMOTHY L. HOTTEL**, DDS, MS, MBA
& **FRANKLIN GARCIA-GODOY**, DDS, MS, PHD, PHD

ABSTRACT: Purpose: To compare fluoride uptake by enamel after applying 1.23% acidulated phosphate fluoride gel to human tooth enamel topically (n=12) or with combined dielectrophoresis and AC electroosmosis (DEP/ACE) at frequencies of 10, 400 and 5,000 Hz (n=12) for 20 minutes. **Methods:** DEP/ACE induced nonuniform electrical fields with three alternating current frequencies to polarize, orient, and motivate fluoride particles. Fluoride concentrations were measured at various enamel depths using wavelength dispersive spectrometry. Data were analyzed by ANOVA/Student-Newman-Keuls post hoc tests ($P \leq 0.05$). **Results:** Fluoride concentrations in the diffusion group were significantly higher than baseline readings at 10, 20 and 50 μm depths. Fluoride concentrations in DEP/ACE-treated teeth were significantly higher than the diffusion group at 10, 20, 50, 100, 200 and 300 μm (ANOVA/Student-Newman-Keuls post hoc, $P < 0.05$). Fluoride uptake with DEP/ACE was substantially higher than diffusion at 10, 20, 50, 100, 200 and 300 μm depths (paired t test, $P < 0.05$). DEP/ACE transported fluoride up to 300 μm deep, whereas conventional fluoride application was comparatively ineffective beyond 20 μm depth ($P < 0.05$). Compared to passive diffusion, fluoride uptake in enamel was significantly higher in the DEP/ACE group at 10, 20, 50, 100, 200 and 300 μm depths ($P < 0.05$). DEP/ACE drove fluoride substantially deeper into human enamel with a difference in uptake 1,575 ppm higher than diffusion at 100 μm depth; 6 times higher at 50 μm depth; 5 times higher at 20 μm depth; and 7 times higher at 10 μm depth. Fluoride levels at 100 μm were equivalent to long-term prophylactic exposure. (*Am J Dent* 2013;26:166-172).

CLINICAL SIGNIFICANCE: Fluoride uptake with dielectrophoresis/AC electroosmosis (DEP/ACE) was significantly greater than topical fluoride application alone (diffusion) and enhanced penetration and absorbed concentration up to 300 μm depth. On average, fluoride concentration with DEP/ACE was 1,575 ppm greater than the diffusion group at 100 μm, reaching appreciable levels (375 ppm) at a depth of 300 μm.

✉: Dr. Chris S. Ivanoff, Department of Bioscience Research, College of Dentistry, University of Tennessee Health Science Center, 875 Union Avenue, Memphis, TN 38163, USA. E-✉: civanoff@uthsc.edu

Introduction

The ability to actuate and control fluid in small amounts with high precision and flexibility is critical to safe and efficient drug delivery. Several micropumping concepts in microfluidics[1,2] could potentially be used to improve drug delivery in dentistry. These systems generate flow by inducing strong electromechanical forces on the fluid element. The forces can be classified as electrohydrodynamic,[3] electroosmotic,[4] and AC electroosmotic,[5-7] among others. More complex fluids, such as colloidal suspensions containing a second phase, including solid/soft particles, can also be manipulated by dielectrophoresis (DEP) upon the application of an external electric field.[8,9]

DEP is the motion of small particles in colloidal suspensions when exposed to non-uniform electric fields, arising from the interaction of the induced dipole on the particle with the applied field.[8-12] DEP has been employed extensively for manipulating particles in biological research, such as in separation,[13-15] trapping,[16] sorting[17,18] and translation[17-22] of cells, viruses, proteins and DNA. DEP research to date has focused on controlling the electromechanical response of the solid particles, but also includes the hydrodynamic interactions between the particles and the surrounding fluid.[23-32]

AC electroosmosis (ACE) is based on the ion migration within a nanometer layer of charges/ions at the interfaces of electrolytes and solids (double layer). This layer of charges will migrate under electric fields tangential to the interface, and because of fluid viscosity, the ion movement carries along its surrounding fluids, leading to fluid motion. The charges in the double layer are induced by AC potentials, and tangential electric fields are also from the same voltage source. Therefore, the changes of polarities in charges and field directions are simultaneous and cancelled out, maintaining steady ion migration and fluid motion. By adjusting the amplitude and frequency of AC signals, a variety of directed surface flows are produced on electrodes to manipulate and transport particles.[24-27,33,34]

These electrokinetic phenomena can be used in combination both to drive fluid flow and manipulate particles. AC electroosmosis can be used to create flow, while DEP can be used to manipulate particles.[33] The phenomenon occurs due to the interaction of induced dipoles with electric fields, and can be used to exhibit a variety of motions including attraction, repulsion and rotation by changing the nature of the dynamic field.

In previous studies, the investigators showed that combined dielectrophoresis and AC electroosmosis (DEP/ACE) could enhance diffusion of fluoride and other agents to penetrate deeper into tooth enamel and in higher concentrations than traditional topical application.[35-37] Wavelength dispersive spectrometry showed that after one 20-minute application of 1.23% acidulated phosphate fluoride (APF) (12,300 ppm fluoride) gel to bovine enamel, DEP/ACE enhanced penetration and increased uptake of fluoride on average by 500% at the depth of 100 μm.[35,36] The amount of fluoride delivered at 50 μm was equivalent to a long-term prophylactic exposure to

fluoride, adding further clinical relevance to the development of a DEP technique as a viable delivery model for dentistry.

In the current study, the investigators explored the efficacy of DEP/ACE to deliver fluoride into human teeth. DEP is used to separate fluoride particles from fluoride gel excipients, concentrate fluoride particles at the enamel surface, and enhance fluoride's diffusion into the enamel. Current diffusion methods are inadequate for effectively transporting therapeutic agents deeper than 20 μm into enamel.[38] Studies have shown that enamel has an approximate 100-250 μm-thick electrical resistant surface layer with very low permeability.[39-41] By applying an AC electrokinetic force, while selectively polarizing and motivating particles with DEP, DEP/ACE may effectively overcome this surface barrier.

Materials and Methods

Electrode design - The DEP/ACE diffusion cell consisted of two arrays of interdigitated (IDE) electrodes fabricated by photolithography. Each IDE array contained 14 pairs of parallel finger microelectrodes, each 35 mm long, 250 μm wide, and 30 μm-thick. The fingers were separated by intervals of 1 mm containing interstitial spaces 0.5 mm wide. The interdigit gaps reduce electrical leakage between electrodes and allow a passage for drug flow. A polyimide coating (thickness 500 nm) prevents electrolysis and corrosion of the electrodes when the device is in contact with the particle suspensions.

A stationary set up was used in which the applied electric signals were controlled by a multi-channel function generator (TGA1244[a]). The applied voltage was $5V_{peak}$, with frequencies continuously cycling at 10, 400 and 5,000 Hz. A digital oscilloscope (Tektronix TDS 3032B[b]) was used to monitor the frequency and waveform of the applied signals during the experiments. The current generated was 0.01-0.03 mA.

Four-point conductivity analysis - The conductivity of the fluoride gel was measured against a range of alternating current frequencies (0.1 to 100,000 Hz) using four-point conductivity analysis.[42] Critical high and low frequencies were then chosen from a Debye plot of the log conductivity (S/cm) values against log frequency (Hz).[35-37] The applied high frequency (5,000 Hz) separates the fluoride particles from the gel excipients and orients the fluoride crystals along the electrode. The optimal low frequency (10 Hz) provides an electromotive force to push the fluoride particles away from the electrode assembly and concentrate the fluoride particles at the enamel surface. An AC electroosmotic frequency (400 Hz) increases the flow of fluoride toward the enamel subsurface by convection.[35,36]

Tooth preparation and fluoride treatment - Twelve virgin human third molars, stored in normal saline solution at 37°C, were cut longitudinally into two halves for a total of 24 specimens. Both halves were coated with nail polish, except for the treatment windows on the buccal enamel. APF gel (PediaGel[c] 1.23% acidulated phosphate fluoride topical fluoride gel) was applied onto the treatment window of both halves. One group of samples was subjected to passive diffusion, while the other was wrapped in the diffusion cell and subjected to DEP/ACE at frequencies of 10, 400 and 5,000 Hz at 37°C and 100% humidity for 20 minutes and wiped with Kimwipe.[d]

Fluoride content analysis - The specimens were cut through the window area, embedded in acrylic resin and polished. The sectioned surface was coated with carbon film, approximately 200 Å thick and subjected to wavelength dispersive spectrometry (WDS) analysis, using a JEOL JXA-8600f[e] electron probe micro-analyzer with 15 nA probe current and 15 kV accelerating voltage. Quantitative analysis of calcium and fluoride was carried out at 10, 20, 50, 100, 200 and 300 μm from the enamel surface. Four measurements with 10 μm spot size were made to obtain an average value at each depth. Quantitative analysis was done in conjunction with atomic number, absorption, and fluorescence matrix correction and calibrated standards, which determined the absolute elemental concentration (weight %) of the elements at designated spots. The standard for both calcium and fluoride was a fluoroapatite (obtained from Durango, Mexico). Two areas were analyzed in each specimen: within the treatment window to determine fluoride content in the treated enamel, and under the nail polish to determine the baseline fluoride content. Fluoride concentration (ppm) at each measurement site was calculated based on weight percent of fluoride and calcium oxide, assuming 37 weight % calcium content in enamel.[43] Baseline fluoride concentration was averaged from both halves. Fluoride uptake was calculated by subtracting the baseline fluoride concentration from the treated site.

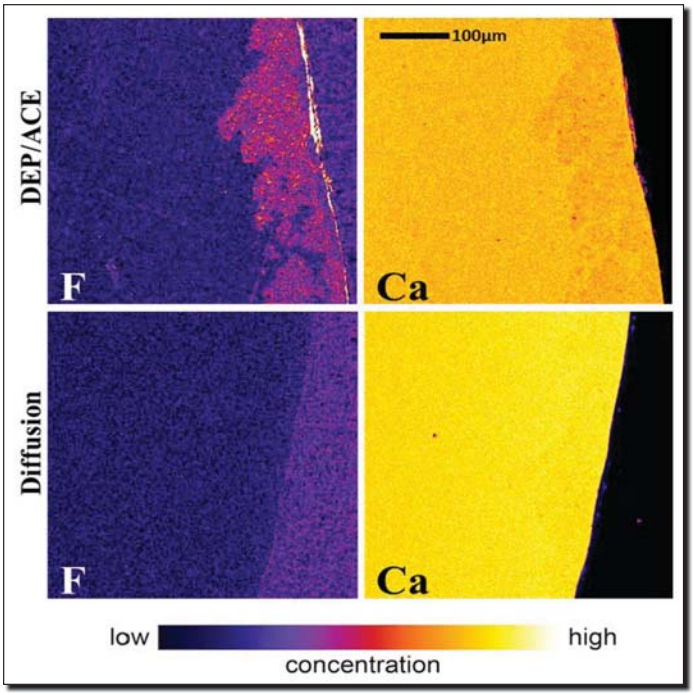

Fig. 1. Wavelength dispersive spectrometry map analysis of fluoride (F) and calcium (Ca) for DEP/ACE and diffusion. The color bar index indicates relative concentrations in arbitrary units within each panel.

Statistical analysis - One-way ANOVA followed by Student-Newman-Keuls post hoc was used to compare the fluoride concentrations between the baseline, diffusion, and DEP/ACE groups at each depth (significance level 0.05). Paired t-test was used to compare the fluoride uptake between the diffusion and DEP/ACE groups at each depth (significance level 0.05).

Results

Spatial distributions of calcium and fluoride from two treatment areas (diffusion and DEP/ACE) with 1 μm step size are shown in Fig. 1, indicating higher fluoride content in the

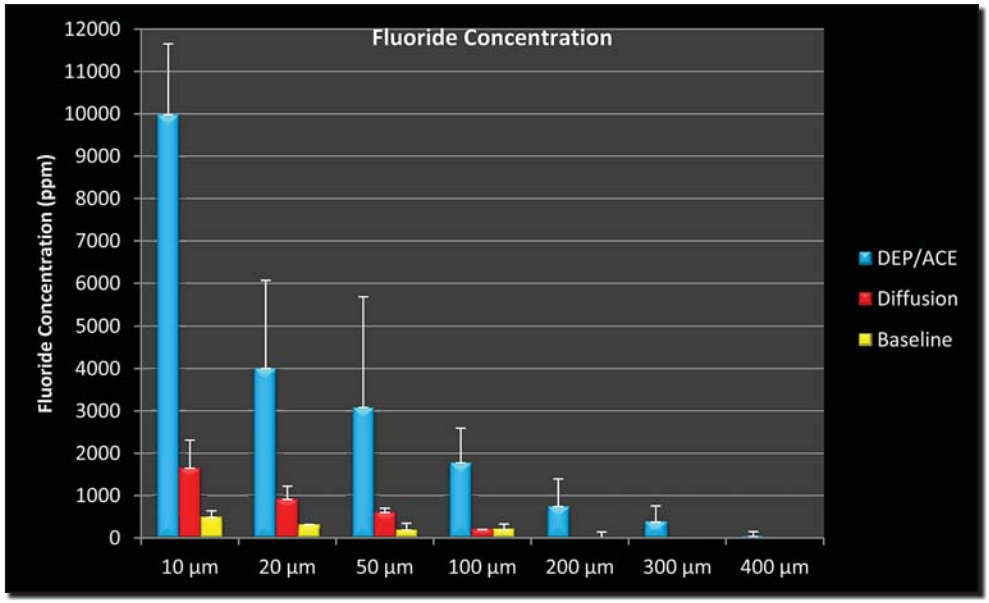

Fig. 2. Fluoride concentrations (mean and standard deviation; ppm) at 10, 20, 50, 100, and 200 µm depths. Significant differences in concentration between DEP/ACE and diffusion groups are indicated at each depth (ANOVA/Student-Newman-Keuls post-hoc; significance level 0.05).

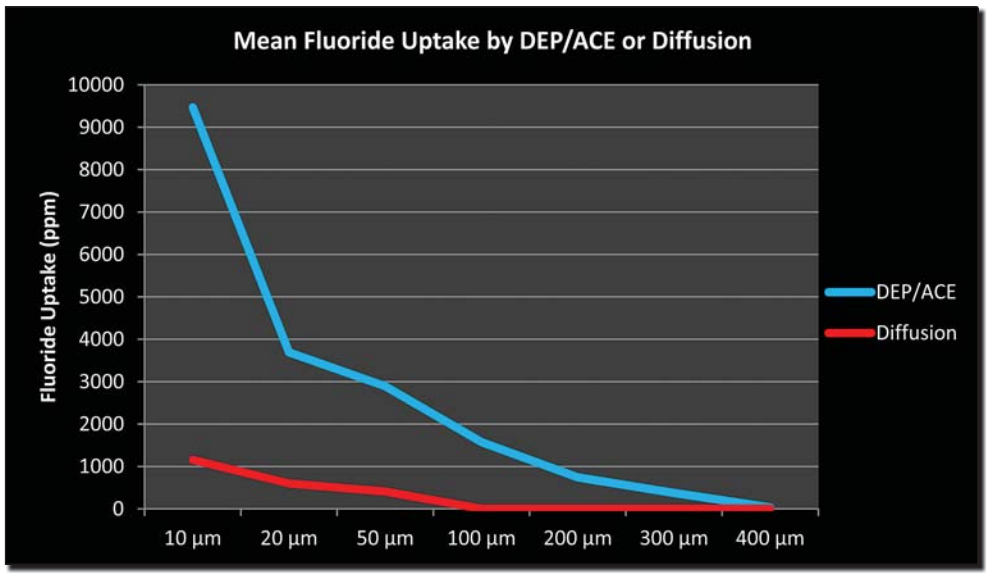

Fig. 3. Mean fluoride uptake in enamel at 10, 20, 50, 100, and 200 µm depths. Significant differences in uptake values between DEP/ACE and diffusion groups are indicated at each depth (paired t-test; P< 0.05).

DEP/ACE group at every depth up to 100 µm. Quantification of fluoride concentration shows that DEP/ACE delivered fluoride up to 300 µm deep, whereas conventional topical fluoride application effectively delivered fluoride to 20 µm depth (P< 0.05). Compared to passive diffusion, fluoride uptake in enamel was significantly higher in the DEP/ACE group at 10, 20, 50, 100, 200 and 300 µm depths (P< 0.05) (Fig. 2). DEP/ACE drove the fluoride substantially deeper into the enamel with a difference in uptake 1,575 ppm higher than diffusion at 100 µm depth (baseline readings were undetected at 100 µm depth); 6 times (582%) higher at 50 µm depth ($[\bar{x}]$=2,892 ppm/409 ppm); 5 (515%) higher at 20 µm depth ($[\bar{x}]$=3,692 ppm/600 ppm); and 7 times (720%) higher at 10 µm depth ($[\bar{x}]$=9,467 ppm/1,154 ppm) (Fig. 3). Average fluoride uptake with DEP/ACE was 742 ppm at 200 µm depth and reached 375 ppm at 300 µm depth during the allotted treatment time.

Discussion

The dielectrophoretic force, F_{DEP}, exerted by the field on a polarizable (dielectric) particle in a surrounding medium, may be approximated by the equation:

$$F_{DEP} = 2\pi r^3 \varepsilon_m \mathrm{Re}[f_{CM}] \nabla E_{rms}^2 \quad (1)$$

where ε_m is the permittivity of the suspending medium; ∇E_{rms}^2 is the root mean square value of the gradient of the squared electric field; Re[f_{CM}] is the real part of the "Clausius-Mossotti" factor given by the equation:

$$f_{CM} = \mathrm{Re}\left[\frac{\varepsilon_p^* - \varepsilon_m^*}{\varepsilon_p^* + 2\varepsilon_m^*}\right] \quad (2)$$

where ε_p^* and ε_m^* are the complex permittivities of the particle and the suspending medium, respectively, defined as $\varepsilon^* = \varepsilon - (j\sigma/\omega)$ where σ and ω are the conductivity and angular frequency of the applied electric field, respectively, and $j = \sqrt{-1}$.[8,12,44]

The frequency dependence of Re[f_{CM}] indicates the force acting on the particle varies with the frequency. Depending on the relative polarizability of the particle with respect to the surrounding medium, the particle will be induced to move either towards a region where the electrical field gradients are the strongest (Re[f_{CM}] > 0) (positive DEP), or towards a region where the electrical field gradients are the weakest (Re[f_{CM}] < 0) (negative DEP). The equation applies to both AC and DC fields.[8,12,44] These dipoles can affect the movement of fluoride molecules in a nonuniform electric field to enhance fluoride's transport into enamel.

The DEP and ACE forces were simulated using COMSOL[f] Multiphysics finite element analysis software version 4.2. Figure 4 shows two sets of simulation results obtained for coplanar and cross-planar excitation of $5V_{peak}$. The periodic nature of the IDE configuration was exploited to simulate a two-dimensional section of the DEP/ACE device consisting of IDE arrays. The simulation region (1.25 mm × 1 mm) is a cross-section of a pair of electrode assemblies (shown midway down both sides of the simulation plots) with interstitial space in the middle region. Each electrode assembly is composed of a top and bottom electrode, separated by a layer of polyimide. The remaining simulation region is filled with water.

The integrated material database was used to induce excita-

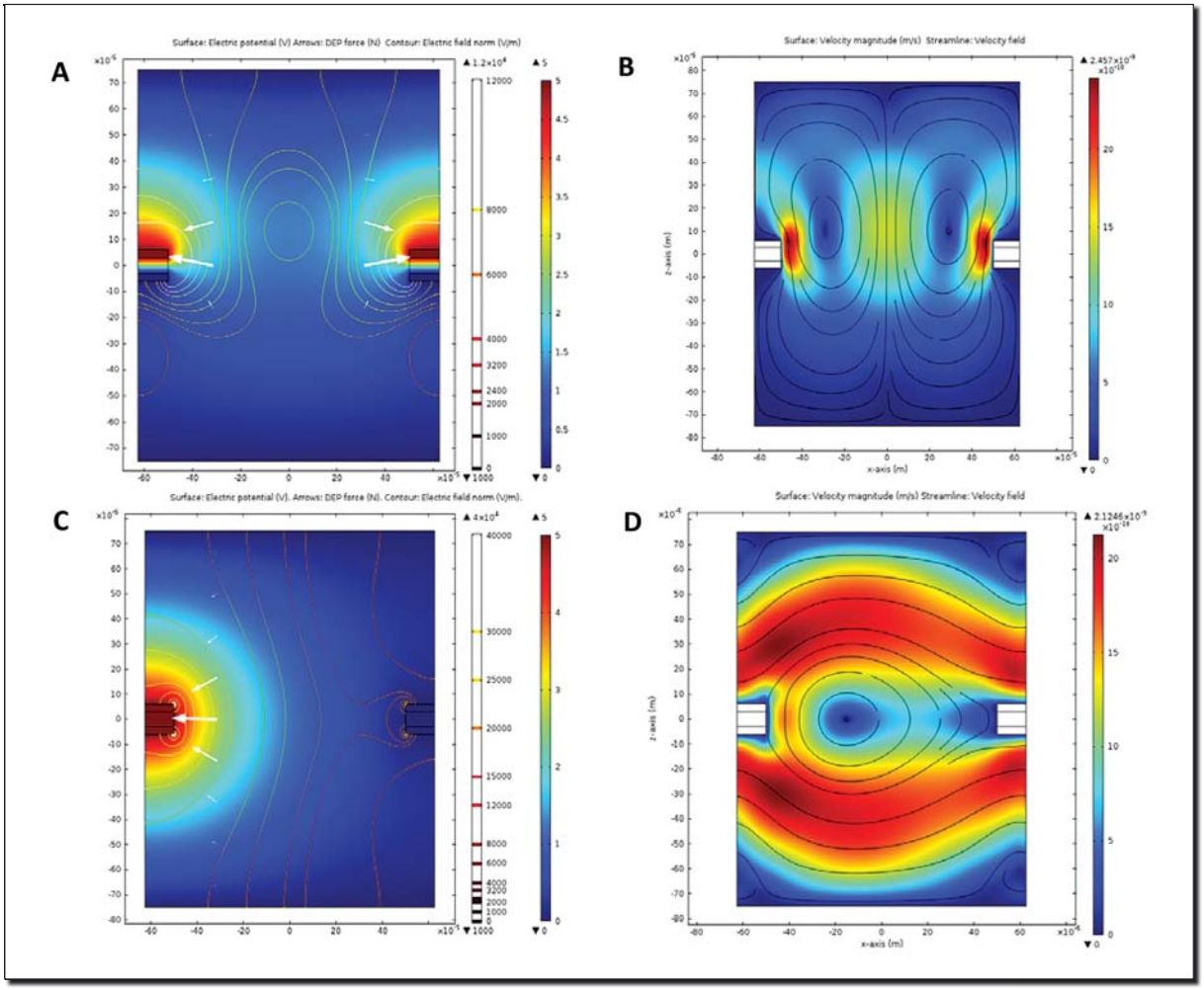

Fig. 4. **A.** Electric potential, DEP force and electric field with coplanar normalized static excitation. **B.** ACE velocity magnitude and field with coplanar normalized static excitation. **C.** Electric potential, DEP force and electric field with cross-planar normalized static excitation. **D.** ACE velocity magnitude and field with cross-planar normalized static excitation.

Table 1. Calculated DEP forces (N) for $5V_{peak}$ excitation.

Probing point measured relative to corner of top electrode assembly	Coplanar excitation		Cross-planar excitation	
	f = 10 Hz	f = 5 kHz	f = 10 Hz	f = 5 kHz
Vertically 1 μm away	-9.190×10^{-12}	9.586×10^{-10}	-4.103×10^{-12}	4.279×10^{-10}
Vertically 5 μm away	-8.123×10^{-13}	8.473×10^{-11}	-9.026×10^{-13}	9.415×10^{-11}
Vertically 100 μm away	-4.513×10^{-15}	4.707×10^{-13}	-9.846×10^{-15}	1.027×10^{-12}
Horizontally 1 μm away	-1.142×10^{-11}	1.191×10^{-9}	-4.308×10^{-12}	4.493×10^{-10}
Horizontally 5 μm away	-1.083×10^{-12}	1.130×10^{-10}	-2.002×10^{-12}	2.088×10^{-10}
Horizontally 100 μm away	-6.203×10^{-15}	6.471×10^{-13}	-1.805×10^{-14}	1.883×10^{-12}

tion at the boundaries of the electrodes, assigning the top and the bottom boundary of the simulation region as terminals, and specifying the boundaries on both sides as periodic. Electric current and fluidic flow physics are included in the simulation with general physics controlled extra fine mesh settings. Plots A and C in Fig. 4 show the electric potential distribution, DEP force and the developed electric fields, while plots B and D depict the ACE velocity magnitudes and fields with the application of a normalized excitation potential between coplanar or cross-planar electrodes.

DEP forces are primarily dominated by conductivity at frequency ranges below 50 MHz.[45] Conductivities of the fluoride gel, measured with a four-point probe instrument, were determined to be 4.4×10^{-4}, 5.5×10^{-3}, and 7.27×10^{-3} (S/cm) at 10, 400 and 5,000 Hz. The corresponding conductivities of water medium were 4.5×10^{-4}, 6.2×10^{-4}, and 6.3×10^{-4} (S/cm), respectively.[46] Assuming the radius of fluoride particles is 5 µm and relative permittivity of the water medium is 80.1,[47] the DEP forces were calculated for an applied potential of $5V_{peak}$ using the simulation results for a number of probing points with respect to the corner of the top electrode in both vertical and horizontal directions as shown in Table 1. As ACE velocities become zero at low and high frequencies, and reach their peak at certain mid-range frequencies,[25] this effect is expected to be most prominent at 400 Hz.

Other electrochemical delivery systems have occasionally been tested to load fluoride into tooth enamel. Until now the results have been disappointing. Although it has been reported

Table 2. Summary of concentrations and net uptake of fluoride at depths 10, 20, 50, 100, 200, and 300 μm with respect to baseline and percent changes within and between DEP/ACE and diffusion groups.

	Fluoride concentration and standard deviation (ppm) at depths 10-400 μm						
Sample	10 μm	20 μm	50 μm	100 μm	200 μm	300 μm	400 μm
Baseline (n=24)	490 (152)	310 (158)	190 (130)	200 (141)	0	0	0
DIF20 (n=12)	1,644 (665)	910 (313)	599 (104)	200 (0)	0	0	0
DEP/ACE20 (n=12)	9,977 (1,676)	4,002 (2,067)	3,082 (2,599)	1,775 (820)	742 (654)	375 (382)	33 (115)
	Mean fluoride uptake (ppm) at depths 10-400 μm						
Sample	10 μm	20 μm	50 μm	100 μm	200 μm	300 μm	400 μm
DIF20 (n=12)	1,154	600	409	0	0	0	0
DEP/ACE20 (n=12)	9,467	3,692	2,892	1,575	742	375	33
Δ (DEP/ACE-DIF)	8,313	3,092	2,383	1,575	742	375	33
ΔDEP/ACE:ΔDIF	720%	515%	582%	n/a	n/a	n/a	n/a
ΔDIF:Base	236%	197%	215%	-	-	-	-
ΔDEP/ACE:Base	2,136%	1,191%	1,522%	798%	n/a	n/a	n/a

that electrophoresis may increase the fluoride content in superficial enamel,[38,48] the advantage over passive diffusion has been inconclusive. While Gedalia et al[49] reported higher fluoride uptake with iontophoresis, Kim et al[50] found no significant difference and Lee et al[38] reported better results with passive diffusion. Based on the results of Gedalia et al,[49] iontophoresis would enhance uptake of fluoride by enamel at 50 μm depth no more than 60% higher than topical application alone. In the current study, DEP/ACE drove the fluoride significantly deeper with an uptake 1,575 ppm higher than diffusion at 100 μm depth and maximum penetration at depth 300 μm. While topical application effectively delivered fluoride up to 20 μm deep, fluoride uptake was 600% higher in the DEP/ACE group at that depth.

Since the validity and significance of the results of this study depend on accurate and relevant measurements, wavelength dispersive spectrometry was used to analyze the elemental compositions of the treated specimens. The detection limit is typically 100 ppm by weight with ± 2% overall analytical accuracy with spatial resolution in the micron range.[51] This technique has previously been used for quantitative analysis of fluoride in residual carious dentin and for calcium and phosphate in demineralized or stained enamel.[35,36,52-54]

Comparison of enamel fluoride concentration between different studies must be carried out with caution, since outcomes may depend on factors like species, tooth stage, and previous fluoride exposure. Nevertheless, it can be noted that the baseline fluoride concentrations in this study were in the same range as values found in the literature. The literature reports that at 10 μm depth, fluoride concentrations range from approximately 170 ppm in porcine enamel to 1,000 ppm in human enamel for a low fluoride area.[55,56] At 20 and 100 μm depths, reported values range between approximately 100-400 and 30-100 ppm respectively.[56,57] This investigation used virgin third molars to overcome contributing factors such as availability of extracted human teeth, as well as natural variations due to age, source, and previous carious experience. Their large size also allowed a paired study design. A 20-minute application time was chosen to assure that the fluoride concentration in the enamel would be measurable.

The diffusion group in the experiments showed a fluoride uptake of 1,154 ppm at 10 μm depth, which decreased to 600 ppm at 20 μm depth. This is comparable with values reported by Wei & Hattab[58] who measured 1,196-1,982 ppm at 10 μm and 565-1,240 ppm at 15 μm in human premolars after 4 minutes gel or foam application. However, fluoride uptake values in the literature vary widely and lower values have also been reported.[56,59] The baseline and passive diffusion results obtained in this study correspond with the same range of values reported in the literature, and thus validate the experimental model used to test the efficacy of DEP/ACE.

Using the DEP/ACE technique, fluoride uptake by human tooth enamel was substantially increased over passive diffusion (Table 2), and significantly higher than both the 351 to 409 ppm fluoride uptake with iontophoresis within the first 50 μm enamel layer, as well as the 113 to 178 ppm uptake by the 50-100 μm enamel layer.[49] The levels of fluoride content after DEP/ACE (Fig. 3) were comparable to, or higher than, concentrations found in enamel after prolonged fluoride exposure in areas with optimally or naturally fluoridated water[60,61] or in mild fluorosis.[62] The substantial difference in fluoride uptake compared to passive diffusion or iontophoresis suggests that DEP/ACE can transport fluoride or other agents significantly better than other existing delivery methods. It is conceivable that the efficacy of DEP/ACE in enamel can be further improved.

The flexible electrode developed for the current application is easily adapted for intraoral use (Fig. 5), adding further clinical relevance to this technique as a viable delivery model for dentistry. Current topical treatments are readily soluble in saliva, quickly dissolving and exhausting their efficacy within 24 hours. DEP/ACE could, however, enhance fluoride delivery into enamel to extend the efficacy window of in-office treatments, promote remineralization and prevent caries. DEP/ACE could potentially transport fluoride into human tooth enamel to essentially create a protected enamel layer 300 μm-thick in one 20-minute application.

In conclusion, fluoride uptake with DEP/ACE was significantly better than diffusion and enhanced penetration and absorbed concentration up to 300 μm depth. On average, fluoride concentration with DEP/ACE was 1,575 ppm greater than the diffusion group at 100 μm, reaching appreciable levels (375 ppm) at depth 300 μm. Topical application was comparatively ineffective beyond 20 μm during the allotted treatment time. Additional research is needed to better understand the optimal conditions and variables that affect the efficacy of DEP/ACE. However, the study confirmed the hypothesis that DEP/ACE could transport more fluoride into human tooth enamel, re-

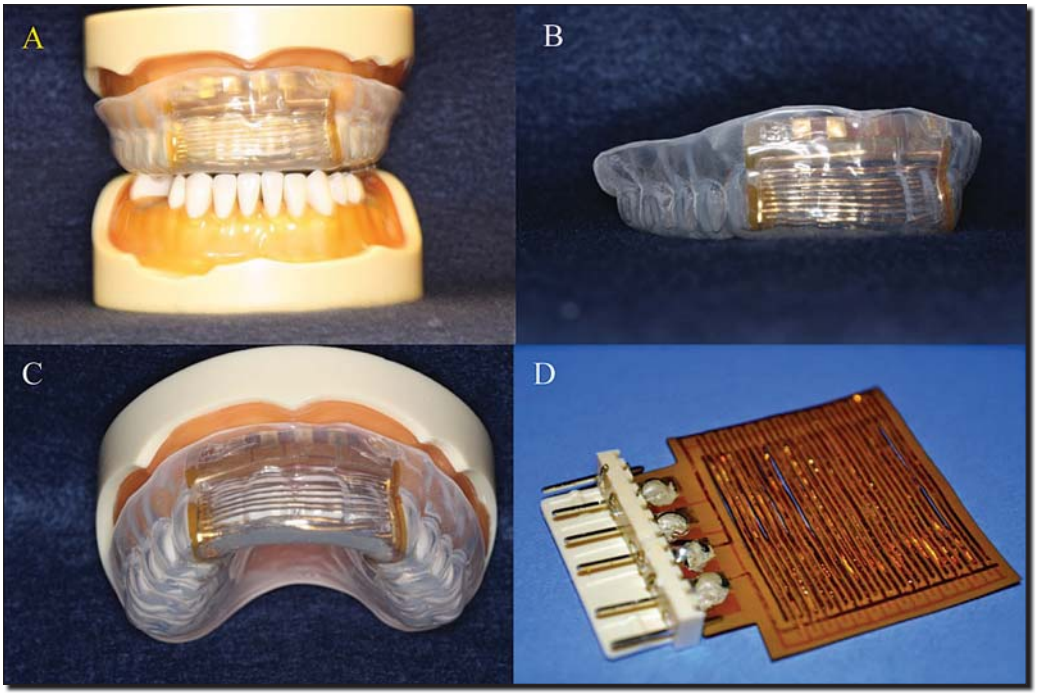

Fig. 5 **A**. DEP/ACE intraordal fluoride delivery system with flexible printed circuit board and polymeric gel tray. **B.** The polymeric tray with embedded electrode is modeled on a conventional fluoride tray. **C.** The tray and electrode conform substantially to shape of the teeth and arch. **D.** DEP/ACE diffusion cell used for bench top lab setting.

sulting in deeper penetration than the diffusion process. The difference of up to a 15-fold increase at depth 100 μm is highly significant when put in the context of existing active delivery methods. Further studies should evaluate the clinical effectiveness of DEP/ACE in enhancing the remineralizing effects of fluoride on human enamel.

a. Thurlby Thandar Instruments Ltd., Cambridgeshire, United Kingdom.
b. Tektronix Inc., Beaverton, OR, USA.
c. Preventive Technologies Inc., Indian Trail, NC, USA.
d. Kimberley-Clark, Neenah, WI, USA.
e. JEOL, Akishima, Tokyo, Japan.
f. COMSOL Inc., Burlington, MA, USA.

Acknowledgements: To Brian Morrow, MS for technical and laboratory assistance and Peter L. McSwiggen, PhD for WDS analysis.

Disclosure statement: The authors declared no conflict of interest. This study was supported by the Alumni Funds of the College of Dentistry, University of Tennessee.

Dr. Ivanoff is Associate Professor, Dr. Hottel is Professor and Dean, and Dr. Garcia-Godoy is Professor and Senior Executive Associate Dean for Research, College of Dentistry, University of Tennessee Health Science Center, Memphis Tennessee, USA. Dr. Bashir is Assistant Professor, Electrical and Computer Engineering, Herff College of Engineering, University of Memphis, Memphis, Tennessee, USA.

References

1. Liu D, Garmiella SV. Microfluidic pumping based on traveling-wave dielectrophoresis. *Nanoscale Microscale Thermophys Eng* 2009;13:109-133.
2. Iverson BD, Garimella SV. Recent advances in microscale pumping technologies: A review and evaluation. *Microfluid Nanofluidic* 2008; 5:145-174.
3. Singhal V, Garimella SV. A novel valveless micropump with electrohydrodynamic enhancement for high heat flux cooling. *IEEE Trans. Advanced Packaging* 2005;28:216-230.
4. Zeng S, Chen CH, Mikkelsen JC, Santiago JG. Fabrication and characterization of electroosmotic micropumps. *Sens Actuator B* 2001; 79:107-114.
5. Islam N, Lian M, Wu J. Enhancing microcantilever capability with integrated AC electroosmosis trapping. *Microfluid Nanofluid* 2007; 3:269-375.
6. Lastochkin D, Zhou R, Wang P, Ben Y, Chang H. Electrokinetic micropump and micromixer design based on ac faradaic polarization. *Appl Phys* 2004;96:1730-1733.
7. Urbanski JP, Thorsen T, Levitan JA, Bazant MZ. Fast ac electro-osmotic micropumps with nonplanar electrodes. *Appl Phys Lett* 2006;89:143508(1-3).
8. Morgan H, Green N. *AC Electrokinetics: Colloids and nano-particles*. Hertfordshire, UK: Research Studies Press Ltd. 2003.
9. Pohl HA. The motion and precipitation of suspensoids in divergent electric fields. *J Appl Phys* 1951;22:869–871.
10. Pohl HA. Some effects of nonuniform fields on dielectrics. *J Appl Phys* 1958;29(8):1182 - 1188.
11. Pohl H. *Dielectrophoresis*. Cambridge, UK: Cambridge University Press, 1978.
12. Burke PJ. Nano-dielectrophoresis: Electronic nanotweezers. In: Nalwa HS. *Encyclopedia of nanoscience and nanotechnology*. Stevenson Ranch, CA, USA: American Scientific 2004;6:623-641.
13. Gascoyne PRC, Vykoukal J. Particle separation by dielectrophoresis. *Electrophoresis* 2002;23:1973-1983.
14. Green NG, Morgan H. Dielectrophoretic separation of nano-particles. *J Phys D: Appl Phys* 1997;30:L41-L44.
15. Morgan H, Hughes MP, Green NG. Separation of submicron bioparticles by dielectrophoresis. *Biophys J* 1999;77:516-525.
16. Hughes MP, Morgan H. Dielectrophoretic trapping of single sub-micrometre scale bioparticles. *J Phys D: Appl Phys* 1998;31:2205-2210.
17. Fiedler S, Shirley SG, Schnelle T, Fuhr G. Dielectrophoretic sorting of particles and cells in a microsystem. *Anal Chem* 1998;70:1909-1915.
18. Holmes D, Morgan H. Cell positioning and sorting using dielectrophoresis. *Eur Cells and Mater* 2002;4:120-122.
19. Washizu M, Kurosawa O, Arai I, Suzuki S, Shimamoto N. Applications of electrostatic stretch-and-positioning of DNA. *IEEE Trans Indust App* 1995;31:447-456.
20. Suehiro J, Pethig R. The dielectrophoretic movement and positioning of a biological cell using a three-dimensional grid electrode system. *J Phys D: Appl Phys* 1998;31:3298-3305.
21. Seger U, Gawad S, Johann R, Bertsch A, Renaud P. Cell immersion and cell dipping in microfluidic devices. *Lab Chip* 2004;4:148–151.
22. Medoro G, Manaresi N, Leonardi A, Altomare L, Tartagni M, Guerrieri R. A lab-on-a-chip for cell detection and manipulation. *IEEE Sens J* 2003;3:317–325.
23. Castellanos A, Ramos A, Gonzalez A, Green NG, Morgan H. Electrohydrodynamics and dielectrophoresis in microsystems: Scaling laws. *J Phys D: Appl Phys* 2003;36:2584-2597.
24. Ramos A, Gonzalez A, Garcia-Sanchez P, Castellanos A. AC electric-field induced fluid flow in microelectrodes. *J Colloid Interface Sci* 1999;217:420-422.
25. Green NG, Ramos A, Gonzalez A, Morgan H, Castellanos A. Fluid flow

induced by non-uniform ac electric fields in electrolytes on micro-electrodes. I. Experimental measurements. *Phys Rev E* 2000;61:4011-4018.
26. Green NG, Ramos A, Gonzalez A, Morgan H, Castellanos A. Fluid flow induced by non-uniform ac electric fields in electrolytes on microelectrodes. II. A linear double-layer analysis. *Phys Rev E* 2000;61:4019-4028.
27. Green NG, Ramos A, Gonzalez A, Morgan H, Castellanos A. Fluid flow induced by non-uniform ac electric fields in electrolytes on micro-electrodes. III. Observation of streamlines and numerical simulation. *Phys Rev E* 2002;66:026305(1-11).
28. Wu J. Interaction of electrical fields with fluids: laboratory-on-chip applications. *IET Nanobiotechnol* 2008;2:14-27.
29. Ramos A, Morgan H, Green NG, Castellanos A. A linear analysis of the effect of Faradaic currents on travelling-wave electroosmosis, *J Colloid Interface Sci* 2007;309:323-331.
30. Wu J. Biased ac electro-osmosis for on chip bioparticle processing. *IEEE Trans Nanotechnol* 2006;5:84-88.
31. Bown MR, Meinhart CD. AC electroosmotic flow in a DNA concentrator. *Microfluid Nanofluid* 2006;2:513-523.
32. Khoshmanesh K, Nahavand S, Baratchi S, Mitchell A, Kalantar-zadeh K. Dielectrophoretic platforms for bio-microfluidic systems. *Biosens Bioelectron* 2011;26:1800–1814.
33. Erickson D, Li D. Analysis of alternating current electroosmotic flows in a rectangular microchannel. *Langmuir* 2003;19:5421-5430.
34. Wu WI, Selvaganapathy PR, Ching CY. Transport of particles and microorganisms in microfluid channels using rectified ac electro-osmotic flow. *Biomicrofluidics* 2011;5:013407(1-12).
35. Ivanoff CS, Hottel TL, Tantbirojn D, Versluis A, Garcia-Godoy F. Dielectrophoretic transport of fluoride into enamel. *Am J Dent* 2011; 24:341-344.
36. Ivanoff CS, Hottel TL, Garcia-Godoy F. Dielectrophoresis: A model to transport drugs directly into teeth. *Electrophoresis* 2012;33:1311-1321.
37. Ivanoff CS, Hottel TL, Garcia-Godoy F. Microhardness recovery of demineralized enamel after treatment with fluoride gel or CPP-ACP paste applied topically or with dielectrophoresis. *Am J Dent* 2012;25:109-113.
38. Lee YE, Baek HJ, Choi YH, Jeong SH, Park YD, Song KB. Comparison of remineralization effect of three topical fluoride regimens on enamel initial carious lesions. *J Dent* 2010;38:166-175.
39. Bjorn H. Electrical excitation of teeth. *Svensk Tandläk Tidskr* 1946;39:Suppl (In Swedish).
40. Ojima K. The enamel reaction on the view of the electric resistance. *Odontology* 1972;60:272-290.
41. Hoppenbrouwers PMM, Scholberg HPF, Borggreven JMPM. Measurement of the permeability of dental enamel and its variation with depth using an electrochemical method. *J Dent Res* 1986;65:154-157.
42. Zhou X, Weston J, Chalkkova E, Hofmann MA, Ambler CM, Allcock. HR, Lvov SN. High temperature transport properties of polyphosphazene membranes for direct methanol fuel cells. *Electrochimica Acta* 2003; 48:2173-2180.
43. Retief DH, Cleaton-Jones PE, Turkstra J, De Wet WJ. The quantitative analysis of 16 elements in normal human enamel and dentine by neutron activation analysis and high-resolution gamma-spectrometry. *Arch Oral Biol* 1971;16:1257-1267.
44. Hughes MP. Nanoparticle manipulation by electrostatic forces. In: Goddard WA, Brenner DW, Lyshevski SE, Iafrate GJ. *Handbook of nanoscience, engineering, and technology*. 2nd ed. Boca Raton, Florida: CRC Press 2007:16.2-16.5.
45. Pethig R. Review article-dielectrophoresis: Status of the theory, technology, and applications. *Biomicrofluidics* 2010;4:022811(1-35).
46. Rusiniak L. Electric properties of water: New experimental data in the 5 Hz – 13 MHz frequency range. *Acta Geophys Pol* 2004;52:363-380.
47. Haynes WM, Lide DR, Bruno TJ. *CRC Handbook of chemistry and physics 2012-2013*. Boca Raton, FL: CRC Press Taylor & Francis Group, 2012.
48. Wagner MJ, Weil TM. Reduction of enamel acid solubility with electrophoretic fluoride applications. *J Dent Res* 1966;45:1563.
49. Gedalia I, Weinman J, Hermel J, Feit D. Fluoride uptake by enamel after immersion in 2% sodium fluoride solution with iontophoresis. *J Dent Res* 1970;49:1555.
50. Kim HE, Kwon HK, Kim BI. Application of fluoride iontophoresis to improve remineralization. *J Oral Rehabil* 2009;36:770-775.
51. Reed SJB. *Electron microprobe analysis*. 2nd ed. Cambridge, Great Britain: Cambridge University Press 1993.
52. Ngo H, Ruben J, Arends J, White D, Mount GJ, Peters MCRB, Faller RV, Pfarrer A. Electron probe microanalysis and transverse microradiography studies of artificial lesions in enamel and dentin: A comparative study. *Adv Dent Res* 1997;11:426-432.
53. Ngo HC, Mount G, Mc Intyre J, Tuisuva J, Von Doussa RJ. Chemical exchange between glass-ionomer restorations and residual carious dentine in permanent molars: An in vivo study. *J Dent* 2006;34:608-613.
54. Tantbirojn D, Douglas WH, Ko CC, McSwiggen PL. Spatial chemical analysis of dental stain using wavelength dispersive spectrometry. *Eur J Oral Sci* 1998;106:971-976.
55. Grobler SR, Joubert JJ. The relative distribution of fluoride in erupted and unerupted enamel of human third molars from a low fluoride area. *Arch Oral Biol* 1988;33:627-630.
56. Richards A, Coote GE, Pearce EIF. Proton probe and acid etching for determining fluoride profiles in porous porcine enamel. *J Dent Res* 1994;73:644-651.
57. Mellberg JR, Nicholson CR, Franchi GJ, Englander HR, Mosley GW. Enamel fluoride uptake and retention from intensive APF gel applications in vivo. *J Dent Res* 1977;56:716-721.
58. Wei SHY, Hattab FN. Enamel fluoride uptake from a new APF foam. *Pediatr Dent* 1988;10:111-114.
59. Dijkman AG, Tak J, Arends J. Comparison of fluoride uptake by human enamel from acidulated phosphate fluoride gels with different fluoride concentrations. *Caries Res* 1982;16:197-200.
60. Nasir HI, Retief DH, Jamison HC. Relationship between enamel fluoride concentration and dental caries in a selected population. *Community Dent Oral Epidemiol* 1985;13:65-67.
61. Li J, Nakagaki H, Tsuboi S, Kato S, Huang S, Mukai M, Robinson C, Strong M. Fluoride profiles in different surfaces of human permanent molar enamels from a naturally fluoridated and a non-fluoridated area. *Arch Oral Biol* 1994;39:727-731.
62. Richards A, Fejerskov O, Bealum V. Enamel fluoride in relation to severity of human dental fluorosis. *Adv Dent Res* 1989;3:147-153.